

# Mineral saturation and scaling tendencies of waters discharged from wells ( $>150\text{ }^{\circ}\text{C}$ ) in geothermal areas of Turkey

Gültekin Tarcan

*Dokuz Eylül University, Geological Engineering Department, Applied Geology Division, Aegean Campus, TR-35100-Bornova-İzmir, Turkey*

Received 1 September 2003; accepted 10 November 2004

## Abstract

Aqueous species distribution was calculated from the chemical composition of water discharges from 27 selected production wells, with reservoir temperatures  $>150\text{ }^{\circ}\text{C}$ , in seven geothermal areas including Kızıldere, Salavatlı, Germencik, Kavaklıdere-Sazdere, Salihli-Caferbeyli, Simav, and Tuzla. Twenty-five of the water compositions are relatively dilute with electroconductivity values of 1826 to 7200  $\mu\text{S}/\text{cm}$  and are dominated by Na (410 to 2027 mg/kg), Cl (45 to 1882 mg/kg), and alkalinity- $\text{CO}_2$  (491 to 2312 mg/kg). Two water samples from Tuzla are highly saline connate waters with Cl of 35 273 to 44 140 mg/kg and Na of 18 200 to 22 250 mg/kg.

Mineral equilibrium modeling indicates that the aquifer waters in these selected geothermal wells, with some exceptions, are oversaturated with respect to calcite, aragonite, and celestite, but undersaturated with respect to gypsum, anhydrite, fluorite, Ca-montmorillonite, anorthite, albite-low, gibbsite, illite, kaolinite, and K-feldspar. The waters are at near saturation with respect to chalcedony, quartz, amorphous silica, dolomite, and strontianite. Calculation of mineral saturation states, geochemical studies, and field observations show that carbonate minerals (calcite, aragonite, and dolomite), amorphous silica, and sulfate minerals (celestite and anhydrite) are most likely to be precipitated as scales in geothermal wells. Assessment of calcite and amorphous silica scaling tendencies for selected well waters indicates that hot injection is favorable for Tuzla well T-2 ( $\sim 50\text{--}170\text{ }^{\circ}\text{C}$ ) and for Kızıldere wells R-1 and KD-6 (around  $100\text{ }^{\circ}\text{C}$ ). For the other wells, cold injection ( $<50\text{ }^{\circ}\text{C}$ ) is favored if calcite and amorphous silica accumulation is to be avoided in injection wells.

© 2004 Elsevier B.V. All rights reserved.

**Keywords:** Turkey; aquifer geochemistry; mineral saturation; scaling; geothermal system

## 1. Introduction

There are eight explored and exploited liquid-dominated geothermal systems in Turkey, with aquifer

temperatures ranging from  $150$  to  $242\text{ }^{\circ}\text{C}$ . All these are linked to the Neogene graben systems within the western Anatolian active tectonic massif, called the Menderes Massif, in western Turkey (Fig. 1). From south to north, the geothermal systems include Denizli Kızıldere, Aydın Germencik, and Aydın

*E-mail address:* [gultekin.tarcan@deu.edu.tr](mailto:gultekin.tarcan@deu.edu.tr).

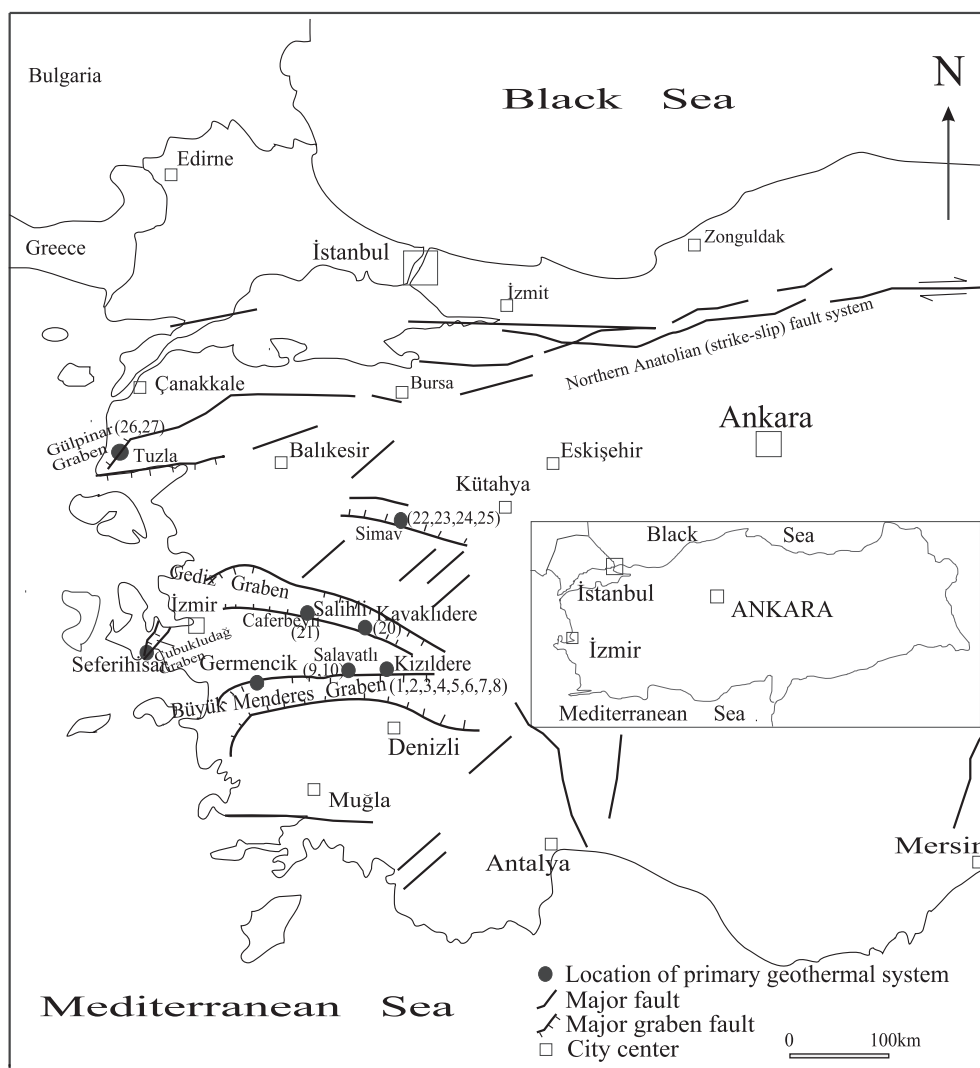


Fig. 1. Location of the primary geothermal areas and wells in Turkey. The numbers in parentheses correspond to sample locality number of wells. Geological structures are modified from Şimşek and Yıldırım (2000), Yılmaz and Karacık (2001), and Bozkurt (2001).

Salavatlı geothermal systems within the Büyük Menderes Graben; İzmir-Seferihisar within the Çubukludağ Graben; Kavaklıdere-Sazdere and Salihli-Caferbeyli within the Gediz Graben; Kütahya Simav within the Simav Graben; and Çanakkale Tuzla in the Gölpinar Graben. The basement in the aforementioned geothermal systems consists of Precambrian to Paleocene (Dora et al., 1997) Menderes Massif rocks, composed of high- to low-grade metamorphics (phyllites, quartz schists, mica schists, gneiss, marbles, dolomitic marbles) and granodiorite.

Menderes Massif rocks are unconformably overlain by Neogene terrestrial sediments consisting of interbedded conglomerate, sandstone, claystone, siltstone, marl, and limestone. Neogene volcanics cover the Menderes Massif rocks and Neogene sediments in some areas. Quaternary alluvium, made up of unconsolidated granular sediments, is also observed in all the areas. Table 1 summarizes the number of wells drilled, minimum and maximum drilled depths, measured down hole temperature ranges, total discharge rate, reservoir and cap rocks, present use, and

Table 1

General data on the primary geothermal systems in Turkey

Sample number	Geothermal system name	NWD	MMDD (m)	MATR ( $t^{\circ}\text{C}$ )	TDR (l/s)	Reservoir rocks and well temperatures	Cap rocks	Present use	References
1–8	Denizli Kızıldere	23	368–2261	195–242	765	1—Pliocene limestone, 148–198 $^{\circ}\text{C}$ ; 2—Palaeozoic to Mesozoic Menderes Massif marble, schist, and quartzite, 200–212 $^{\circ}\text{C}$ ; 3—Palaeozoic to Mesozoic Menderes Massif quartzite and schist, 242 $^{\circ}\text{C}$	Pliocene intercalated claystone, sandstone, conglomerate)	Electricity (20 MWe), dry ice and $\text{CO}_2$ production	Şimşek, 1985; MTA, 1996; Şimşek et al., 2000
9–10	Aydın Salavatlı	2	962–1510	162–172	186	Palaeozoic to Mesozoic Menderes Massif quartzite and schist	Pliocene intercalated claystone, sandstone, conglomerate	Spa, greenhouse heating	MTA, 1996; Karamanderesi, 1997a; Vengosh et al., 2002
11–19	Aydın Germencik	9	200–2398	203–232	840	1—Miocene conglomerate, 203–214 $^{\circ}\text{C}$ 2—Palaeozoic to Mesozoic Menderes Massif marble, schist and quartzite, 216–232 $^{\circ}\text{C}$	Pliocene intercalated claystone, sandstone, conglomerate	Spa, greenhouse heating	MTA, 1996; Şimşek et al., 2000; Filiz et al., 2000; Vengosh et al., 2002
20	Kavaklıdere-Sazdere	1	1447	182	12	Palaeozoic to Mesozoic Menderes Massif marble, schist, and quartzite, 182 $^{\circ}\text{C}$	Neogene intercalated claystone, sandstone, conglomerate	No use	Karahan et al., 2003; Tarcan et al., 2002
21	Salihli-Caferbeyli	1	1189	155	2	Palaeozoic to Mesozoic Menderes Massif marble, schist, and quartzite, 155 $^{\circ}\text{C}$	Neogene intercalated claystone, sandstone, conglomerate	No use	MTA, 1996; Karamanderesi, 1997b; Tarcan et al., 2000
22–25	Kütahya Simav	12	65–958	97–170	359	1—Neogene Naşa basalts; 2—Mesozoic limestone of Kırkbudak fm; 3—Palaeozoic to Mesozoic Simav marble, schist, and gneiss	Neogene clayey sediments	Spa, district heating, greenhouse heating	MTA, 1996; Gemici and Tarcan, 2002
26–27	Çanakkale Tuzla	14	81–1020	90–174	120	1—Lower Miocene rhyolitic tuffs, ignimbrites, latitic and rhyolitic lavas; 2—Kestanbol granite and granodiorite, 28 Ma	Miocene tuffitic claystone and conglomerates	Spa	Karamanderesi, 1986; MTA, 1996; Mützenber, 1997; Şener and Gevrek, 2000
	İzmir Seferihisar	10	151–2000	78–153	300	Bornova melange sandstone, shale, limestone, chert, mafic volcanics, and serpentinite, 153 $^{\circ}\text{C}$	Neogene intercalated claystone, conglomerate, and sandstone	Spa	Eşder, 1990; Tarcan and Gemici, 2003

All the systems are linked to young tectonics. Sample numbers correspond to locality numbers shown in Fig. 1. NWD: number of wells drilled; MMDD (m): minimum and maximum drilled depth; MATR ( $t^{\circ}\text{C}$ ): measured down hole temperature range; TDR (l/s): total discharge rate. The numbers 1 and 3 for under reservoir rocks (in seventh column) reflect the shallowest rocks and deepest rocks, respectively.

references for the primary geothermal systems in Turkey.

Exploration of Kızıldere began in 1968, and to date, 23 deep wells have been drilled. The wells produce from a reservoir with a maximum temperature of 242 °C (Şimşek, 1985; MTA, 1996; Şimşek et al., 2000). Eight wells are utilized for the 20 MWe single flash power plant and for liquid CO<sub>2</sub> and dry ice production. The two wells in the Aydın Salavatlı system were drilled within low resistivity zones and discharge 170 °C aquifer waters (MTA, 1996; Karamenderesi, 1997a). The Aydın Germencik geothermal system has the second highest temperature reservoir at 232 °C in Turkey, after Kızıldere (242 °C). Nine wells have been drilled in the area with measured well deep temperatures of 200–232 °C (MTA, 1996; Filiz et al., 2000; Şimşek et al., 2000). At present, the wells are not being used, but installation of a power plant is being planned for future.

Manisa Kavaklıdere-Sazdere is a recently discovered geothermal system, in the Gediz Graben with a maximum well deep temperature of 182 °C (Tarcan et al., 2002; Karahan et al., 2003). A well drilled in the Manisa Salihli-Caferbeyli geothermal system has a maximum temperature of 155 °C (Karamenderesi, 1997b; Tarcan et al., 2000). However, a low discharge rate of 2 l/s, suggesting low permeability, has deterred economic use of this well. Thermal waters from springs and deep wells in Kütahya Simav geothermal system, discharging waters from a 170 °C reservoir, are used for balneological purposes and district heating purposes (MTA, 1996; Gemici and Tarcan, 2002). There are a number of thermal springs and 12 shallow wells apart from the two deep wells in the Çanakkale Tuzla geothermal area (MTA, 1996; Mützenber, 1997). Here, thermal fluids are hosted in a 28 Ma granodiorite (Fytikas et al., 1976) and Lower Miocene volcanic rocks (Şener and Gevrek, 2000). A number of thermal springs and 10 geothermal wells having depths of 151–2000 m are located in the Çubukludağ Graben in İzmir-Seferihisar (Eşder, 1990; Tarcan and Gemici, 2003). A well (CM-3) in this area intersected a maximum temperature of 153 °C at depth. However, chemical analyses of discharge waters are not available, and therefore this system is not represented in this study.

The purpose of this study is to examine and to review the hydrogeochemical data and the state of mineral saturation in the aquifer of the primary geothermal systems in Turkey. For this purpose, a total of 27 wells were selected to assess aquifer geochemistry. In this study, special emphasis is put on the study of aquifer chemistry and the evaluation of scaling problems. WATCH (Arnórsson et al., 1982; Bjarnason, 1994), PhreeqCi (Parkhurst and Appelo, 1999), and AquaChem-Version 3.7.42 (Calmbach, 1997) computer codes were used to evaluate the geochemical properties of water samples and to calculate aqueous speciation in the aquifer waters.

## 2. Hydrogeochemical outline

Thermal discharge waters in Kızıldere, Salavatlı, Kavaklıdere-Sazdere, Caferbeyli, and Simav have electrical conductivity values between 1826 and 7200 µS/cm and are relatively dilute (Table 2). However, two wells in Tuzla discharge (26 and 27 in Table 2) extremely saline brine with chloride concentrations as high as 44140 mg/kg. Mützenber (1997) noted that the chemical and isotopic composition of the Tuzla waters indicate the presence of a fossil altered sea water (connate water), which is diluted with up to 70% fresh meteoric water. In the triangular Cl–SO<sub>4</sub>–HCO<sub>3</sub> diagram, water compositions in the inland eastern geothermal systems of Kızıldere, Salavatlı, Kavaklıdere-Sazdere, Caferbeyli, and Simav have HCO<sub>3</sub>/Cl ratios >4.0 (Fig. 2). In the western geothermal systems, located nearer the sea, the HCO<sub>3</sub>/Cl ratios are <2. Thermal brine in Tuzla plots in Cl corner. In Germencik, wells producing from aquifers shallower than 1300 m have lower HCO<sub>3</sub>/Cl ratios at 1.1. However, the deepest well has a higher HCO<sub>3</sub>/Cl ratio of ~2.0 (Fig. 2). Reservoir rocks in the selected geothermal areas consist of metamorphics (gneiss, schist, and marble) and sedimentary rocks including limestone. Waters derived from such rock formations are naturally rich in calcium, sodium, and bicarbonate ions due to water–rock interaction. As shown in Table 2, B contents of the waters from selected wells reach peak values of 86.6 mg/kg in KG-1 well waters in Kavaklıdere-Sazdere (number 20 in Table 2). This

Table 2

Chemical analyses of the selected water samples from wells in primary Turkish geothermal fields

No	Location, well	Date drilled	Depth (m)	Flow (l/s)	Aq. T (t °C)	EC (µS/cm)	pH	Alkalinity (CO <sub>2</sub> )	SiO <sub>2</sub>	Na	K	Mg	Ca	Li	B	F	Cl	SO <sub>4</sub>	Al	Sr
1 <sup>a</sup>	Kızıldere, R-1	1998	2261	198	242		8.34	1963	508	1525	203	0.05	0.53			26.6	132	526	2.40	0.26
2 <sup>b</sup>	Kızıldere, KD-6	1970	851	40	196	5830 <sup>c</sup>	7.76	1695	310	1134	131	0.27	1.15	3.96 <sup>d</sup>	20	17.3	46	644	0.15	0.41 <sup>e</sup>
3 <sup>a</sup>	Kızıldere, KD-13	1971	760	40	195	5940 <sup>c</sup>	9.63	1391	305	1214	132	0.18	0.42	4.09 <sup>d</sup>		17.2	100	337	0.55	0.18
4 <sup>b</sup>	Kızıldere, KD-15	1971	510	92	205	5890 <sup>c</sup>	9.30	1559	400	1335	154	0.24	0.95	3.62 <sup>d</sup>	27	23.4	58	704	0.25	
5 <sup>b</sup>	Kızıldere, KD-16	1973	667	151	211	5835 <sup>c</sup>	8.12	1854	393	1245	151	0.29	3.65	4.43 <sup>d</sup>	27	23.8	49	656	0.30	0.40 <sup>f</sup>
6 <sup>c</sup>	Kızıldere, KD-20	1986	810	78	201	6180 <sup>c</sup>	8.92	1408	367	1330	140 <sup>d</sup>	0.15	1.60	4.58 <sup>d</sup>	24	22.5 <sup>d</sup>	140	676		0.33 <sup>e</sup>
7 <sup>c</sup>	Kızıldere, KD-21	1985	898	66	202	5940 <sup>c</sup>	9.02	1452	387	1550	140 <sup>d</sup>	0.24	1.80		25	21.0 <sup>d</sup>	140	772		
8 <sup>a</sup>	Kızıldere, KD-22	1986	888	100	202	5830 <sup>c</sup>	9.12	1417	316	1282	144	0.15	0.47			18.5	100	504	0.55	0.19
9 <sup>g</sup>	Salavatlı, AS-1	1987	1510	94	162	3400	7.10	1832	100	1100	100	3.60	20	3	54	12.5	228	153		1.0 <sup>f</sup>
10 <sup>g</sup>	Salavatlı, AS-2	1987	962	92	172	4600	7.67	2042	178	1100	90	1.10	14	6	42		233	170		
11 <sup>g</sup>	Germencik, ÖB-1	1982	1000	35	203		8.50	907	140	1355	45	16	50		45	2.4	1586	37		
12 <sup>g</sup>	Germencik, ÖB-2	1982	976	25	231	7200	9.00	1201	160	1830	189	<0.1	1.6		71	8.3	1359	71		
13 <sup>g</sup>	Germencik, ÖB-3	1983	1197	65	230	7100	8.78	1118	55	1775	170	0.5	1.6		68	8.0	1818	74		2 <sup>f</sup>
14 <sup>g</sup>	Germencik, ÖB-4	1984	285	180	213	5400	7.71	1039	53	1420	135	1.7	12		55	7.3	1500	37		
15 <sup>g</sup>	Germencik, ÖB-5	1984	1302	65	221	3000	8.43	1065	209	1387	128	6.8	8.4		56		1454	46		
16 <sup>g</sup>	Germencik, ÖB-6	1984	1100	140	221	6200	8.70	1078	41	1775	180	<0.1	3.6		74		1882	64		
17 <sup>g</sup>	Germencik, ÖB-7	1985	2398	65	203	4200	7.53	1325	214	1100	132	6.1	19		56		855	51		
18 <sup>g</sup>	Germencik, ÖB-8	1986	200	120	220	6600	8.87	1031	286	1550	15	243	8				1528	45		
19 <sup>g</sup>	Germencik, ÖB-9	1986	1465	145	224	6500	8.60	1089	286	1750	105	1.2	4.8		68	7.3	1819	133		11.0 <sup>f</sup>
20 <sup>h</sup>	Kavaklıdere-Sazdere, KG-1	2002	1447	12	182	6020	8.31	2312	261	2027	79	3.1	12.8	5.28	86.6		165	1843	1.08	2.32
21 <sup>i</sup>	Salihli-Caferbeyli, SC-1	1990	1189	2	155	2700	7.80	1430	214	680	70	6.1	42	0.12	67	3.1	115	34		
22 <sup>j</sup>	Simav-Eynal, EJ-1	1990	725	72	163	2300	8.74	528	364	506	55	4.9	11.6	0.42	2.7		80	471	0.36	
23 <sup>j</sup>	Simav-Eynal, E-6	1990	169	60	160	2280	8.84	512	349	532	62	5.8	6.4	0.42	1.1		80	456	0.36	
24 <sup>j</sup>	Simav-Eynal, E-8	1996	225	50	150	2300	9.20	491	338	523	58	4.6	8.4	0.42	1.1		81	446	0.38	
25 <sup>j</sup>	Simav-Çitgöl Ç-2	1996	134		162	1830	7.91	595	250	410	39	5.6	26	0.09	0.2		65	393	0.11	
26 <sup>k</sup>	Çanakkale-Tuzla, T-1	1982	814	31	174	57000	7.00	40	123	22250	2125	101	5716	74	36.0	4.3	44140	264		139
27 <sup>k</sup>	Çanakkale-Tuzla, T-2	1983	1020		168	62600	6.00	62	159	18200	2780	68	2781	23.4	30.1	2.0	35273	209		130

Concentrations are in milligram per kilogram unless otherwise stated.

Blanks show no data. Aq. T (t °C): measured down hole temperature; pH: standard unit at 25 °C. Sample numbers correspond to locality numbers shown in Fig. 1.

<sup>a</sup> Giese (1997).<sup>b</sup> Lindal and Kristmannsdóttir (1989).<sup>c</sup> Satman et al. (1999).<sup>d</sup> Yıldırım et al., 1997.<sup>e</sup> ENEL (1989).<sup>f</sup> Vengosh et al. (2002).<sup>g</sup> MTA (1996).<sup>h</sup> Tarcan et al. (2002).<sup>i</sup> Karamandere (1997b).<sup>j</sup> Gemici and Tarcan, 2002.<sup>k</sup> Mützenberg, 1997.

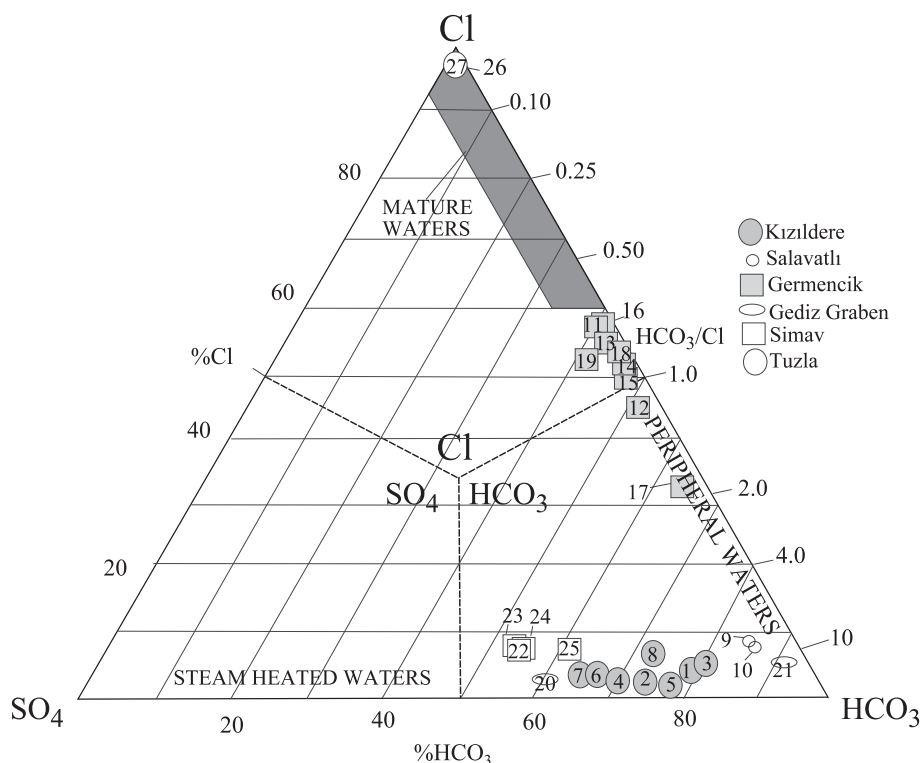


Fig. 2. Discharge water composition from selected Turkish geothermal wells plotted in a Cl–HCO<sub>3</sub>–SO<sub>4</sub> diagram (modified from Giggenbach, 1991). Sample numbers are the same as in Table 2.

is the highest value among the Turkish geothermal areas.

### 3. Chemical geothermometry

Although the maximum down hole temperatures of all the selected well waters for this study were already measured, their aquifer temperatures were recalculated by chemical geothermometers to compare both results and to examine the applicability of the various geothermometers. Chemical geothermometers are based on temperature dependent water–rock equilibria and give the last temperature of water–rock equilibrium attained in the aquifer (Nicholson, 1993). However, during ascent towards the surface, thermal waters may mix with various types of cooler ground waters. Application of some geothermometers to mixed waters may provide poor results. The Na–K–Mg diagram (Fig. 3) proposed by Giggenbach (1988) is often used to evaluate aquifer temperatures and to

recognize waters, which have attained equilibrium with the host lithology and waters affected by mixing and/or reequilibration at low temperatures along their circulation path. Immature waters plot rather close to the Mg corner. The waters that plot between the full equilibrium and immature water curves may result from mixing a fully or partly equilibrated water with cold immature water. All the Simav waters (22 to 25 in Table 2) and the waters from SC-1 (sample 21) and ÖB-8 (sample 18) wells fall into the immature field. Since these waters do not attain equilibrium, the evaluation of equilibrium temperatures is not reliable, and the results obtained by the cation geothermometers should be only tentative. Waters from ÖB-1 (sample 11), ÖB-5 (sample 15), ÖB-7 (sample 17), and AS-1 (sample 9) are located in the field of partially equilibrated waters near the boundary of immature waters. Data points from the Kızıldere area plot on or near the curve of fully equilibrated waters and reflect reservoir temperatures ranging between 220 and 250 °C. The rest plot on

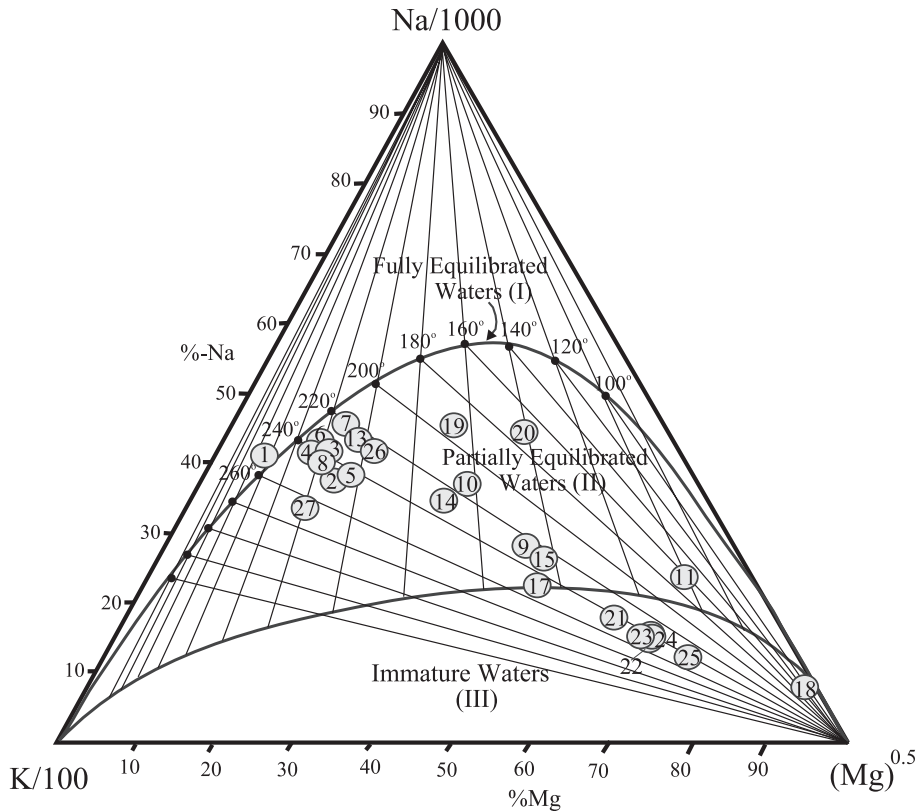


Fig. 3. Water composition of selected well discharges in Turkey plotted in a Na–K–Mg diagram (Giggenbach, 1988). Sample numbers are the same as in Table 2.

the field of partially equilibrated waters and may result from mixing fully or partly equilibrated water with cold immature water.

Table 3 shows the results of the some chemical geothermometer applications. Comparing the measured aquifer temperatures (maximum down hole temperature), it is on opinion that the Na–K–Ca and Na–K–Ca (Mg corrections) temperatures are mostly higher than measured down hole well temperatures. This can partly be caused by calcium loss from the water during boiling through calcite and/or aragonite precipitations. Part of the difference could be due to an indication of higher temperatures at deeper levels. Geothermometers based on Mg/Li and Na/Li (Kharaka and Mariner, 1989) ratios are both unreliable, which give very low temperatures for Caferbeyli (sample 21) and Simav (samples 22 to 25), whereas give mostly higher results than measured down hole temperatures for Kızıldere (2–6), Salavatlı (9–10), and

Tuzla (samples 26 and 27). However Mg/Li equation gives the best match with measured temperature of the well KG-1 (sample 20). The chalcedony, quartz (steam loss), and Na/K (Truesdell, 1976; Fournier, 1979) geothermometers generally provide results similar to measured well temperature. Especially, the temperatures obtained from chalcedony geothermometers in waters from Kızıldere (samples 1 to 8) and Kavaklıdere (sample 20) wells are very close to the measured temperature, whereas quartz geothermometers give a little high temperature. Silica geothermometers compared with measured temperatures suggest mixing and dilution of waters at Salavatlı, Germencik, and Tuzla, due to the fact that measured temperatures are higher than silica geothermometers. These results coincide with the results obtained from the Na–K–Mg diagram. Silica and all the Na/K geothermometers show that the main reservoir was not intersected at system Simav–Eynal. Because



Table 3

Calculated aquifer temperatures of waters from selected wells in primary geothermal areas of Turkey

No.	Name	Measured (t °C)	SiO <sub>2</sub> <sup>a</sup> Chalcedony	SiO <sub>2</sub> <sup>a</sup> Quartz	SiO <sub>2</sub> <sup>a</sup> Quartz Steam loss	Mg/Li <sup>b</sup>	Na/Li <sup>b</sup>	Na/K <sup>c</sup>	Na/K <sup>d</sup>	Na/K <sup>e</sup>	Na–K– Ca <sup>f</sup> $\beta=1/3$	Na–K–Ca <sup>d</sup> Mg-corrections
1	Kızıldere, R-1	242	247	254	227			221	267	243	290	
2	Kızıldere, KD-6	196	196	212	194	228	218	204	252	230	261	258 (R=0.7)
3	Kızıldere, KD-13	195	195	211	193	242	216	197	246	224	271	
4	Kızıldere, KD-15	205	221	233	210	227	202	204	252	230	267	
5	Kızıldere, KD-16	211	219	231	209	233	219	210	257	234	252	247 (R=0.6)
6	Kızıldere, KD-20	201	212	225	205	255	217	193	243	221	254	
7	Kızıldere, KD-21	202	218	230	208			177	228	208	245	238 (R=0.5)
8	Kızıldere, KD-22	202	198	213	195			201	249	227	273	
9	Salavatlı, AS-1	162	110	137	133	152	202	178	229	209	211	167 (R=7.7)
10	Salavatlı, AS-2	172	150	172	162	212	249	167	219	200	208	198 (R=2.9)
11	Germencik, ÖB-1	203	132	157	149			93	150	138	152	63 (R=26.5)
12	Germencik, ÖB-2	231	142	165	156			191	241	220	260	
13	Germencik, ÖB-3	230	77	106	106			183	234	213	254	253 (R=0.9)
14	Germencik, ÖB-4	213	75	104	105			182	233	213	225	208 (R=3.3)
15	Germencik, ÖB-5	221	190	207	190			179	230	210	226	137 (R=13.1)
16	Germencik, ÖB-6	221	62	92	94			189	239	218	248	
17	Germencik, ÖB-7	203	164	184	172			208	256	233	230	158 (R=10.4)
18	Germencik, ÖB-8	220	189	206	189			25	82	75	114	
19	Germencik, ÖB-9	224	189	206	189			139	193	177	210	197 (R=3.3)
20	Kavaklıdere, KG-1	182	181	199	183	180	200	105	161	148	178	143 (R=8.7)
21	Caferbeyli, SC-1	155	164	184	172	44	78	191	240	219	202	137 (R=11.4)
22	Simav-Eynal, EJ-1	163	211	225	204	79	138	197	246	224	212	111 (R=16.8)
23	Simav-Eynal, E-6	160	207	221	201	76	136	205	253	230	224	100 (R=20.0)
24	Simav-Eynal, E-8	150	204	219	199	80	137	199	248	226	217	114 (R=16.6)
25	Simav-Çitgöl Ç-2	162	177	196	181	39	85	182	233	213	192	105 (R=16.7)
26	Tuzla, T-1	174	124	149	143	226	215	183	233	213	218	210 (R=2.4)
27	Tuzla, T-2	168	142	165	156	177	160	239	282	256	254	240 (R=2.6)

Sample numbers are as in Table 2 corresponding to locality numbers shown in Fig. 1. Measured down hole temperatures are shown in the third column for comparison.

Blanks reflect no data or not applicable.

<sup>a</sup> Fournier (1977).

<sup>b</sup> Kharaka and Mariner (1989).

<sup>c</sup> Truesdell (1976).

<sup>d</sup> Fournier and Potter (1979).

<sup>e</sup> Fournier (1979).

<sup>f</sup> Fournier and Truesdell (1973).

measured temperatures are lower than silica and Na/K geothermometers.

#### 4. Mineral saturation and scaling potential

Prediction of the scaling tendencies from geothermal waters is important in evaluating the production characteristics of geothermal aquifers and for taking necessary precautions to prevent or control scale formation. Assessment of scaling tendencies

involves calculation of the saturation state of the scale forming minerals. PhreeqCi computer code (Parkhurst and Appelo, 1999) was used to calculate aqueous speciation distribution in the aquifer waters. Activity coefficients of aqueous species are defined with the Davies equation for high-salinity waters and WATEQ Debye–Hückel equation (Truesdell and Jones, 1974) for more dilute thermal waters. The activity products for the following minerals were calculated: albite-low, amorphous silica, anhydrite, anorthite, aragonite, Ca-montmorillonite, calcite, celestite, chalcedony, dolo-



mite, fluorite, gibbsite, gypsum, illite, kaolinite, K-feldspar, quartz, strontianite. All of the minerals except for anorthite have been identified as hydrothermal minerals in the primary Turkish geothermal areas (Karamenderesi, 1986; MTA, 1996; Şener and Gevrek, 2000; Vengosh et al., 2002; Karamenderesi and Helvacı, 2003). The activity products of anorthite were also calculated, since it is one of the end-member feldspars. Comparison between the solubility constant ( $K$ ) and the activity product ( $Q$ ) permits evaluation of whether the water is undersaturated ( $Q < K$ ), at equilibrium with ( $Q = K$ ) or oversaturated ( $Q > K$ ) with a particular mineral. The solubility product ( $\log Q$ ) of each aforementioned mineral, together with the solubility constant ( $K$ ) curves, is plotted against temperature in Fig. 4. Departures from equilibrium for each mineral are given in terms of saturation index (SI),  $\log(Q/K)$  in Table 4, as well as average and mean departures from equilibrium and standard deviation of the mean departure. Negative  $\log(Q/K)$  values in Table 4 indicate undersaturation and positive values oversaturation. An average departure of near zero from equilibrium indicates that aquifer waters are at equilibrium with mineral. The mean value, on the other hand, gives the mean departure (absolute value) from equilibrium.

All of the waters are oversaturated with respect to calcite and aragonite except for the Kızıldere R-1 well (1 in Table 2), which is slightly undersaturated. These two types of  $\text{CaCO}_3$  show very similar scatter on the  $\log Q$  versus temperature diagrams. Equilibrium with calcite and/or aragonite is rapidly attained at relatively high temperatures. Hence, geothermal waters would be very close to calcite and/or aragonite saturation. Aquifer waters of Simav, Kavaklıdere, Caferbeyli, Salavatlı, and some Germencik samples are oversaturated with respect to dolomite. However, waters from Kızıldere, Germencik, and Tuzla are undersaturated, up to four orders of magnitude. The three  $\text{SiO}_2$  minerals amorphous silica, chalcedony, and quartz show similar scatter. The results depicted in Fig. 4 for amorphous silica show mostly slightly negative  $\log(Q/K)$  values at 150–182 °C, but positive  $\log(Q/K)$  values at >182 °C. In contrast, chalcedony and quartz have slightly positive  $\log(Q/K)$  values. Both silica polymorphs are mostly oversaturated above 190 °C but closely approach equilibrium below 190 °C. The only aquifer water, which is heavily

undersaturated with respect to chalcedony and quartz, is that of Germencik well ÖB-15 (no. 15 in Fig. 4). This is probably an artifact due to faulty data.

All of the waters are undersaturated with respect to gypsum up to seven orders of magnitude. Another  $\text{CaSO}_4$  mineral, anhydrite, is slightly undersaturated in most water samples except in Tuzla (26, 27 in Table 2) and Kavaklıdere (20 in Table 2), where there is slight oversaturation. Fluorite is slightly to heavily undersaturated in all the aquifer waters. Aquifer waters are undersaturated with respect to Ca-montmorillonite, except for well R-1 in Kızıldere (Fig. 4), which is oversaturated up to 12 orders of magnitude. Similarly, all the waters are undersaturated with respect to illite, except for waters from wells R-1 and KD-15, which are slightly oversaturated. Departures and standard deviations are given in Table 4. The two Sr minerals, celestite and strontianite, show different scatter patterns. The waters closely approach equilibrium with strontianite. However, celestite is slightly to moderately oversaturated for all the examined aquifer waters, except for the Salavatlı well AS-1, which is slightly undersaturated. The albite-low, anorthite, and K-feldspar minerals—three end members of feldspar—show similar scatter. Albite-low and K-feldspar are undersaturated for most waters except for some Kızıldere wells (1, 3, 4, and 8), where they are moderately oversaturated. The results depicted in Fig. 4 for kaolinite show mostly moderately to heavily negative  $\log(Q/K)$  values. The water from well R-1 is oversaturated with respect to kaolinite. Waters from other wells are undersaturated.

The saturation states of thermal waters with respect to selected minerals suggest that carbonate minerals (calcite, aragonite, and some dolomite) are most likely to be precipitated as scales from the primary geothermal waters of Turkey during geothermal exploitation and well production. Additionally silica polymorphs (amorphous silica, quartz, and chalcedony) and sulfate minerals (celestite and some anhydrite) seem to be precipitated at various temperatures during production applications. These results coincide with field observations of scaling tendencies in Kızıldere wells. Mineralogical studies of scales from wells at Kızıldere suggest the presence of calcite, aragonite, and amorphous silica (Şamilgil and Arda, 1977). Furthermore, Giese et al. (1998) carried out mineralogical studies on well KD-22, and they noted

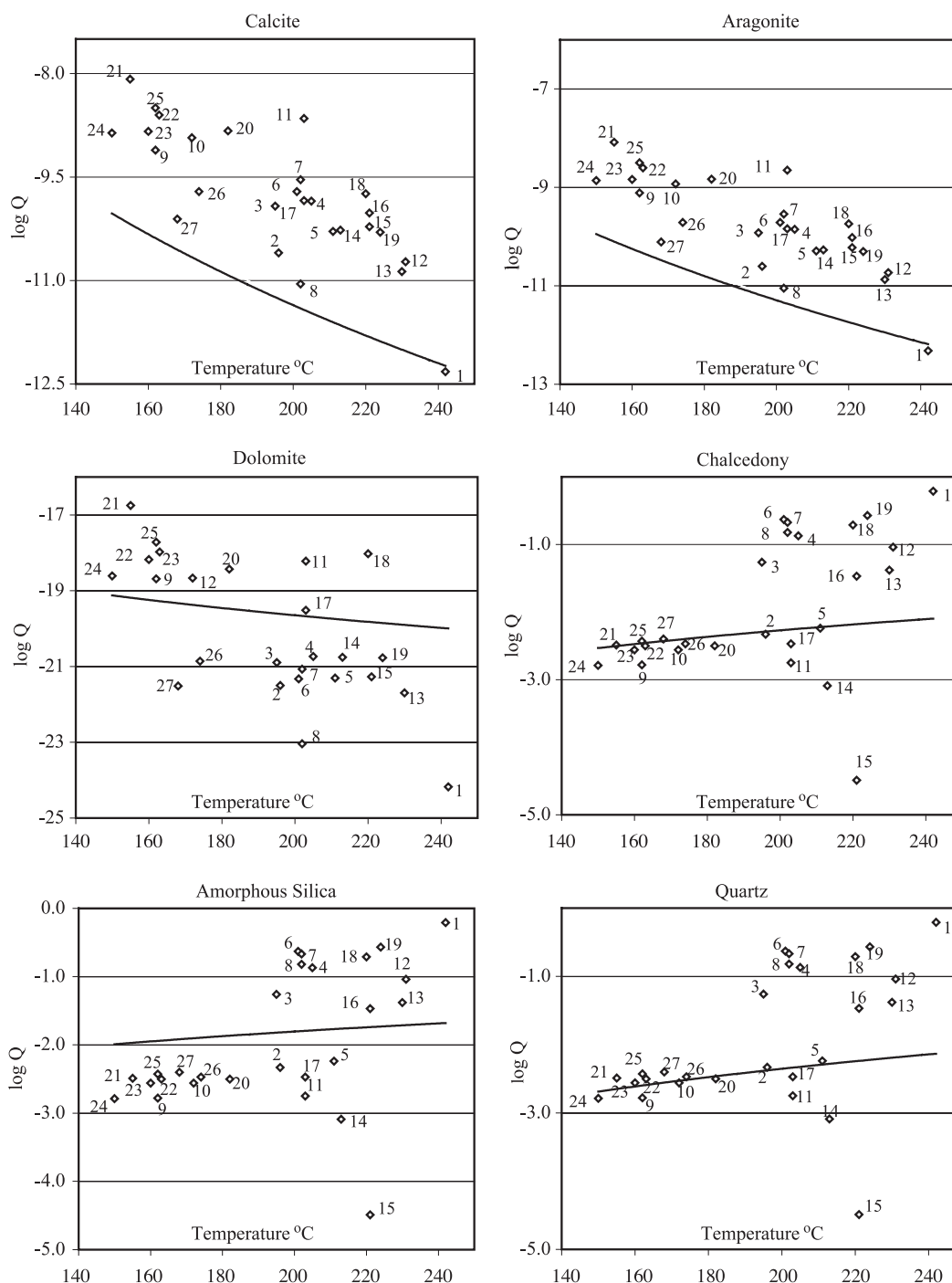


Fig. 4. The saturation state of waters from selected geothermal wells in primary Turkish geothermal systems with respect to selected minerals. The solid curves represent the solubility constant ( $\log K$ ) of each mineral. Numbers are the same as Table 2.

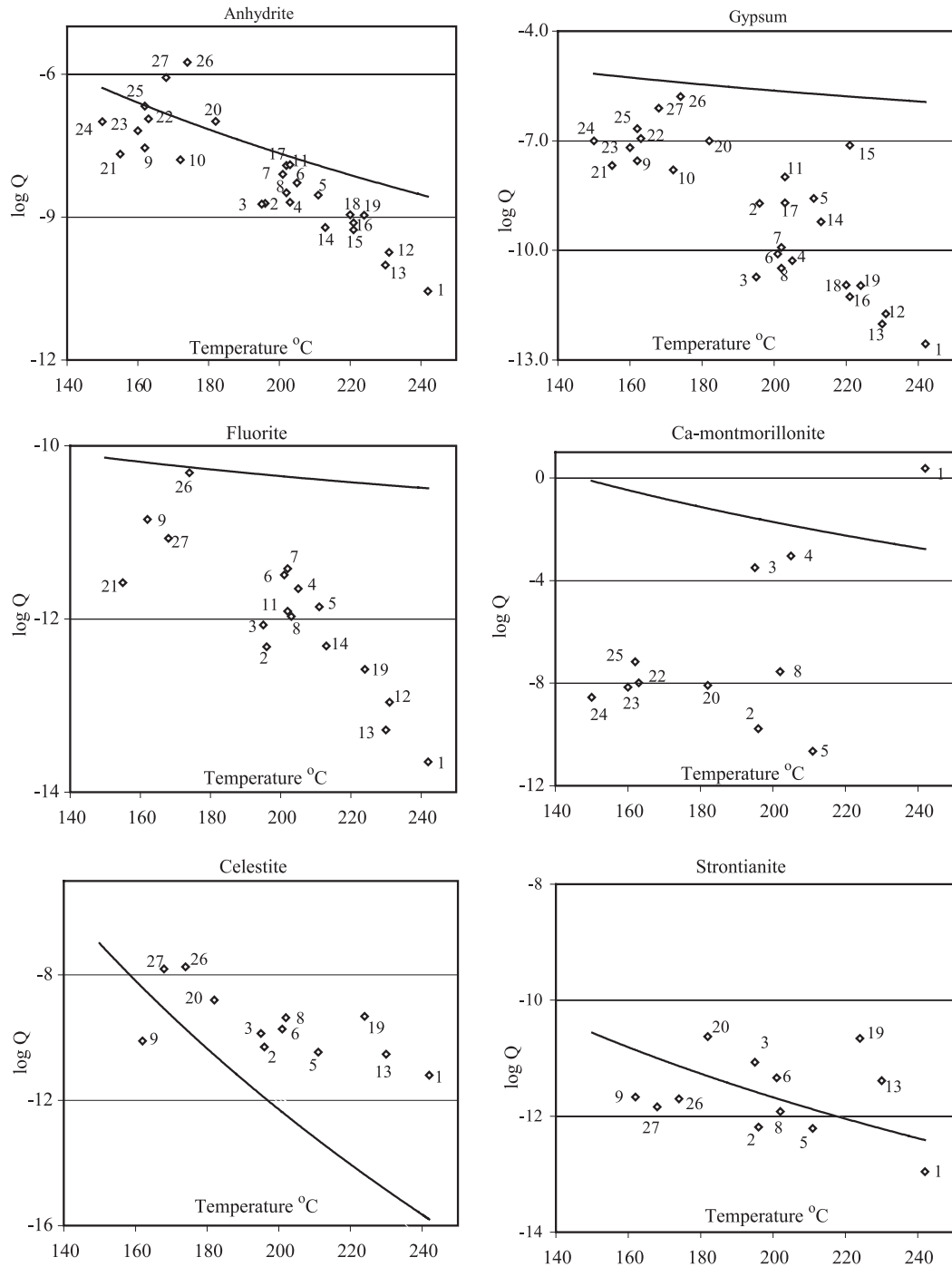


Fig. 4 (continued).

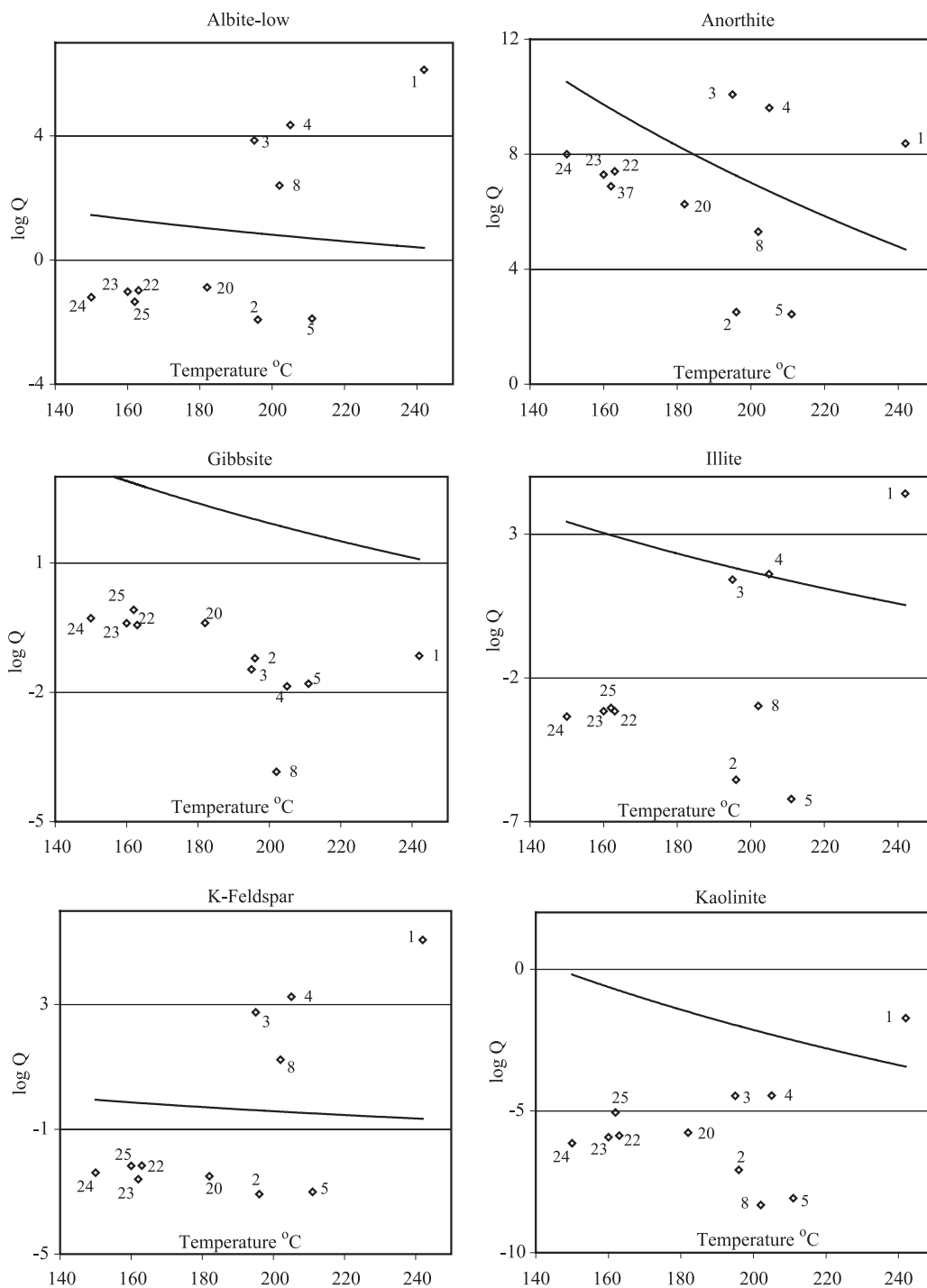


Fig. 4 (continued).

Table 4

Statistical departures from equilibrium for each mineral with respect to SI (log  $Q/K$ ) values

Mineral	Formula <sup>a</sup>	Average departure	Mean departure	Standard deviation
Albite-low	NaAlSi <sub>3</sub> O <sub>8</sub>	−0.292	2.741	3.140
Amorphous Silica	SiO <sub>2</sub>	−0.117	0.813	0.975
Anhydrite	CaSO <sub>4</sub>	−0.680	0.501	0.676
Anorthite	CaAl <sub>2</sub> Si <sub>2</sub> O <sub>8</sub>	−1.140	2.322	2.885
Aragonite	CaCO <sub>3</sub>	1.375	0.434	0.588
Ca-Montmorillonite	Ca <sub>0.165</sub> Al <sub>2.33</sub> Si <sub>3.67</sub> O <sub>10</sub> (OH) <sub>2</sub>	−5.421	2.960	3.782
Calcite	CaCO <sub>3</sub>	1.442	0.435	0.590
Celestite	SrSO <sub>4</sub>	2.070	1.257	1.825
Chalcedony	SiO <sub>2</sub>	0.357	0.790	0.960
Dolomite	CaMg(CO <sub>3</sub> ) <sub>2</sub>	−0.504	1.453	1.694
Fluorite	CaF <sub>2</sub>	−0.520	0.638	0.842
Gibbsite	Al(OH) <sub>3</sub>	−3.220	0.597	0.928
Gypsum	CaSO <sub>4</sub> ·2H <sub>2</sub> O	−3.355	1.557	1.788
Illite	K <sub>0.6</sub> Mg <sub>0.25</sub> Al <sub>2.3</sub> Si <sub>3.5</sub> O <sub>10</sub> (OH) <sub>2</sub>	−4.109	3.167	3.890
Kaolinite	Al <sub>2</sub> Si <sub>2</sub> O <sub>5</sub> (OH) <sub>4</sub>	−4.061	1.682	2.311
K-feldspar	KAlSi <sub>3</sub> O <sub>8</sub>	−0.181	2.719	3.108
Quartz	SiO <sub>2</sub>	0.450	0.769	0.948
Strontianite	SrCO <sub>3</sub>	−0.005	0.631	0.736

<sup>a</sup> Taken from PhreeqCi (Parkhurst and Appelo, 1999).

that scaling at depths from 550 to 200 m comprise nearly 90% calcite and 10% aragonite, but in upper part of well, the amount of aragonite increases to nearly 70%. L ndal and Kristmannsd ttir (1989) showed that samples of suspended materials and scales taken from a pipeline from well KD-6 contain Ca as the main component, with trace concentrations of Sr, Ba, Si, Fe, K, Al, and S. They also found, besides aragonite, considerable amounts of silica (10–15 weight percent of the total scale) in a sample of scale collected in K zildere in a pipeline connecting a well separator and a silencer. Also, chemical analyses of scales for five samples (in weight percent) from wells at K zildere made by MTA yielded the following results ( amilgil and Arda, 1977): 60.0–78.2% CaCO<sub>3</sub>, 15.7–19.52% SrCO<sub>3</sub>, 0.19–0.57% BaCO<sub>3</sub>, 0.2–1.8% MgCO<sub>3</sub>, 0.2–18.1% SiO<sub>2</sub>, and traces of aluminum, sodium, and iron.

High strontium contents in scales show possible deposition of celestite or strontianite. The mineralogical and chemical data on scales in K zildere support the results of mineral saturation studies performed in this study, predicting scale deposition of calcite, aragonite, amorphous silica, and celestite. However, some minerals, i.e., kaolinite, albite-low, and K-feldspar are oversaturated in some of the selected

wells for this study. Yet, albite, kaolinite, K-feldspar, and many other silicates and even quartz and chalcedony do not form as scale in Turkish geothermal wells. The reason is assumed to be slow kinetics for the precipitation of these minerals. Amorphous silica, calcite, and anhydrite, on the other hand, can readily precipitate from oversaturated solution ( rn rsson, 2000a).

Studies on scaling have mostly been focused on the K zildere Geothermal Area by previous workers (L ndal and Kristmannsd ttir (1989); G kg z, 1998; Giese et al., 1998; Tarcan, 2001). L ndal and Kristmannsd ttir (1989) noted that rapid precipitation of calcium carbonate from the discharge water occurs just after steam separation and that there appears to be a high risk of siliceous deposits from the water by cooling below about 100  C. G kg z (1998) stated that the boiled water from K zildere wells is supersaturated with respect to calcite even at low temperatures. Tarcan (2001) claims that cold injection is favorable for K zildere if calcite and amorphous silica deposition is to be avoided in injection wells. However, scaling is a problem encountered in all the principal geothermal areas in Turkey. The most common scales in most geothermal systems in the world involve calcite and amorphous silica ( rn rsson, 1989;  rmannsson,

1989; Kristmannsdóttir, 1989). The discussion below is confined to these types of scales.

#### 4.1. Calcite and amorphous silica scaling tendencies in production wells

In order to demonstrate calcite and amorphous silica-scaling tendencies in production wells, chemical data from wells used in this study were selected on the basis of locations (Kızıldere, wells R-1 and KD-22; Germencik, wells ÖB-2 and ÖB-5; Salavatlı, well AS-

1; Gediz Graben, wells KG-1 and SC-1; Simav, EJ-1; Tuzla, T-1). Fig. 5 shows the calculated saturation states of calcite and amorphous silica scaling for the waters in these nine wells during single-step adiabatic boiling, assuming maximum degassing (i.e., equilibrium distribution is attained for all gases present between the aqueous and steam phases). All the selected waters show a change towards calcite over-saturation during the early stages of boiling (steam flashing) except for R-1 well discharges. These results reflect the temperature dependence of CO<sub>2</sub> gas

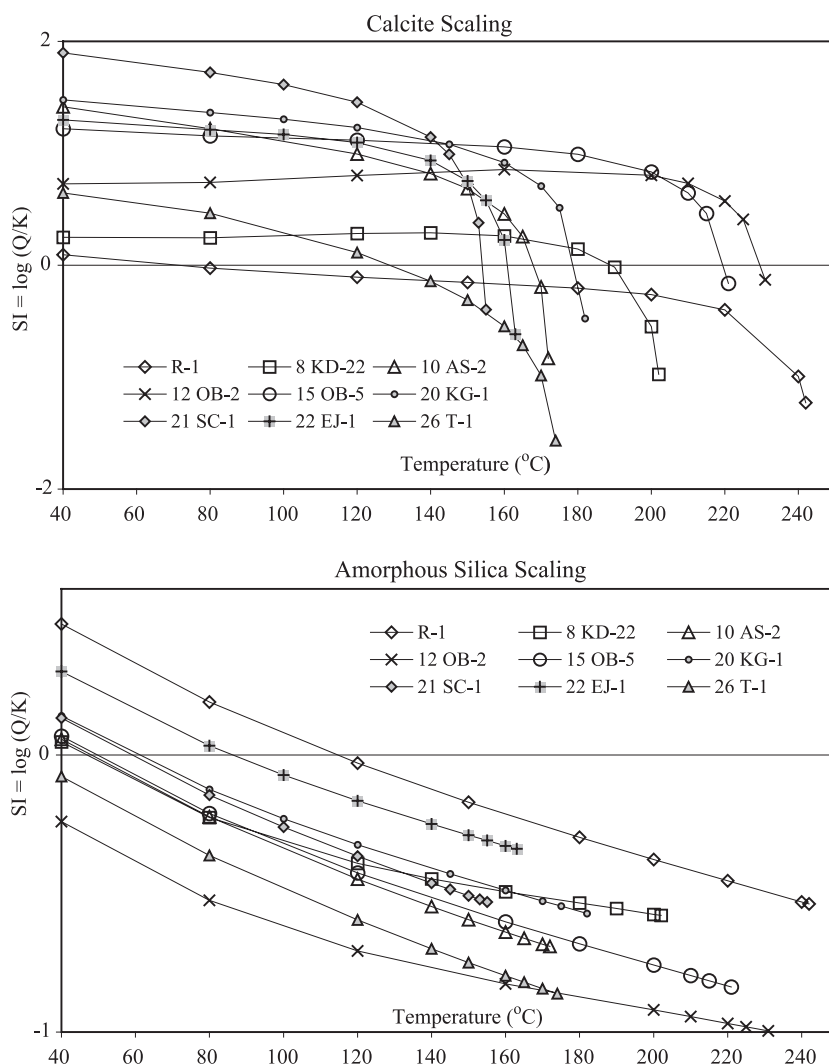


Fig. 5. Changes in the state of calcite and amorphous silica saturation in waters from selected geothermal wells in Turkey upon adiabatic boiling. Numbers are the same as Table 2.

solubility (i.e., degassing is more effective at lower water temperatures). The degree of calcite oversaturation increases during the early stages of boiling of the water in these wells, because the effect of degassing dominates over the effect of retrograde calcite solubility (Arnórsson, 2000a). At lower temperatures, the relative effect of retrograde calcite solubility becomes more important. In high-temperature wells, calcite scaling has only been troublesome during steam flash in the well bore. Precipitation begins at the depth of flashing and becomes most intense above that level. In Kızıldere, the first level of boiling in well KD-22 is at 600 m below the wellhead, and significant scale formation begins at a depth of 550 m (Giese et al., 1998). At shallower depths, it decreases and may disappear altogether below the wellhead. Geothermal aquifer water compositions are always close to calcite saturation. Boiling causes a drastic decrease in  $\text{CO}_2$  partial pressures, which leads to calcite oversaturation and precipitation.

Cooling, resulting from boiling, causes the water to become oversaturated with respect to amorphous silica, because its solubility decreases with decreasing temperature. For the wells ÖB-2, T-1, the saturation indices with respect to amorphous silica do not cross zero (equilibrium line) at the temperatures considered. Waters from wells R-1 and EJ-1 are undersaturated and cross the zero line at  $\sim 115$  and  $\sim 85$  °C, respectively (Fig. 5). The other wells cross the zero line between  $\sim 45$  and  $\sim 65$  °C. Therefore, amorphous silica scaling appears to be a risk below  $\sim 115$  °C for well R-1,  $\sim 85$  °C for well EJ-1, and under  $\sim 65$  °C for the other wells except ÖB-2 and T-1, which have no risk at all. In geothermal waters above 150 °C, silica concentrations are usually controlled by quartz solubility (Arnórsson, 2000a). Cooling induced by boiling and accompanied increase in aqueous silica concentrations by steam loss causes the water to become silica oversaturated. However, quartz precipitation is sluggish, and silica is only removed from solution at an appreciable rate if the solution becomes oversaturated with amorphous silica, particularly when this oversaturated water comes into contact with air (Arnórsson, 2000a). The temperature, at which amorphous silica saturation is attained in high-temperature well waters, depends on the aquifer temperature, the change in pH of the water as it boils and possible separation of the water and steam phases

in the aquifer flowing towards the well. Ionization of dissolved silica, caused by pH increase, lowers the temperature at which amorphous silica saturation is reached. The rate of amorphous silica precipitation is positively related to water temperature, the degree of water oversaturation, and water salinity (Arnórsson, 1989).

#### 4.2. Calcite and amorphous silica scaling tendencies in reinjection wells

It is an important practice to dispose of waste geothermal water by reinjection, either into shallow or deep drillholes, usually peripheral to production zones. If the water is disposed of by reinjection into shallow drillholes, it may be expected to cool further in the formation. On the other hand, if injected into deep wells, it may gain heat. A decrease in temperature may bring about oversaturation with respect to some minerals, thus creating a tendency for them to precipitate from the water in the formation. It is important to assess the state of mineral saturation in waste geothermal water that is intended to be disposed of by reinjection in order to find out the optimum temperature for injection (Arnórsson, 2000a). Fig. 6 shows the calculated state of calcite saturation for the waters in all the geothermal wells in this study assuming conductive cooling (according to WATCH modeling). For these computations, deep-water compositions of waters at 100 °C obtained from boiling assumptions are used. All the well waters show moderate to strong oversaturation with respect to calcite at any temperature (even  $< 100$  °C) except for R-1, KD-6, AS-1, and T-2 wells. Wells R-1 and KD-6 waters are oversaturated above  $\sim 100$  °C. Wells AS-1 and T-2 waters are oversaturated above  $\sim 20$  and  $\sim 170$  °C, respectively. Fig. 7 shows the calculated saturation states of amorphous silica assuming conductive cooling. All the wells show similar trends against temperature. Kızıldere and Salavatlı waters are oversaturated below the temperature intervals between 20 and 120 °C. Wells ÖB3, ÖB4, and ÖB6 waters do not cross the zero line at any temperature. The other Germencik well waters are oversaturated below the temperatures between  $\sim 30$  and  $\sim 70$  °C. The other wells show oversaturation below the temperatures between  $\sim 30$  and  $\sim 90$  °C. Silica scaling tendencies increase with decreasing aquifer temperature. Calcite and amor-



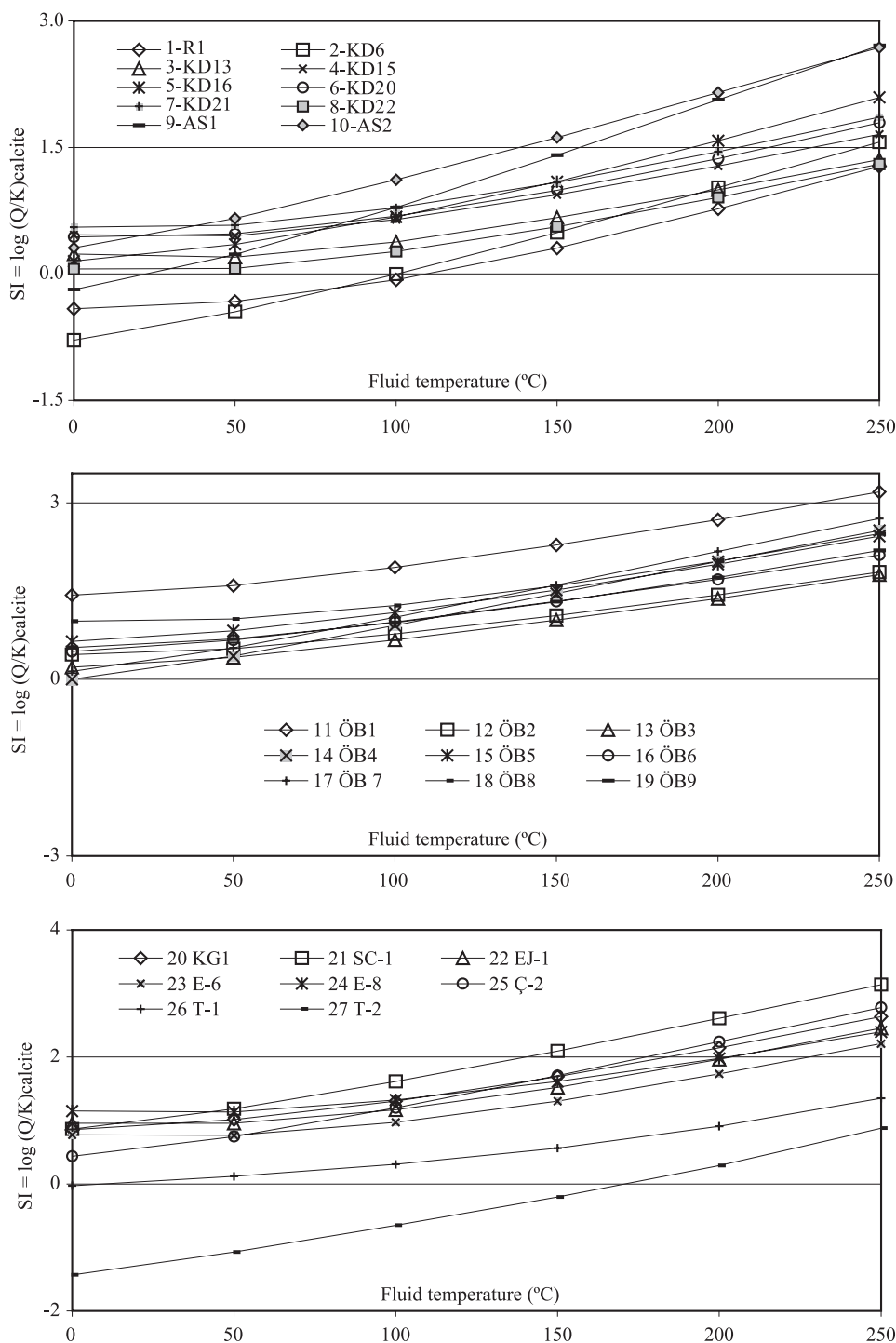


Fig. 6. Changes in the state of calcite saturation in waters from selected geothermal wells in Turkey upon conductive cooling. Numbers are as Table 2.

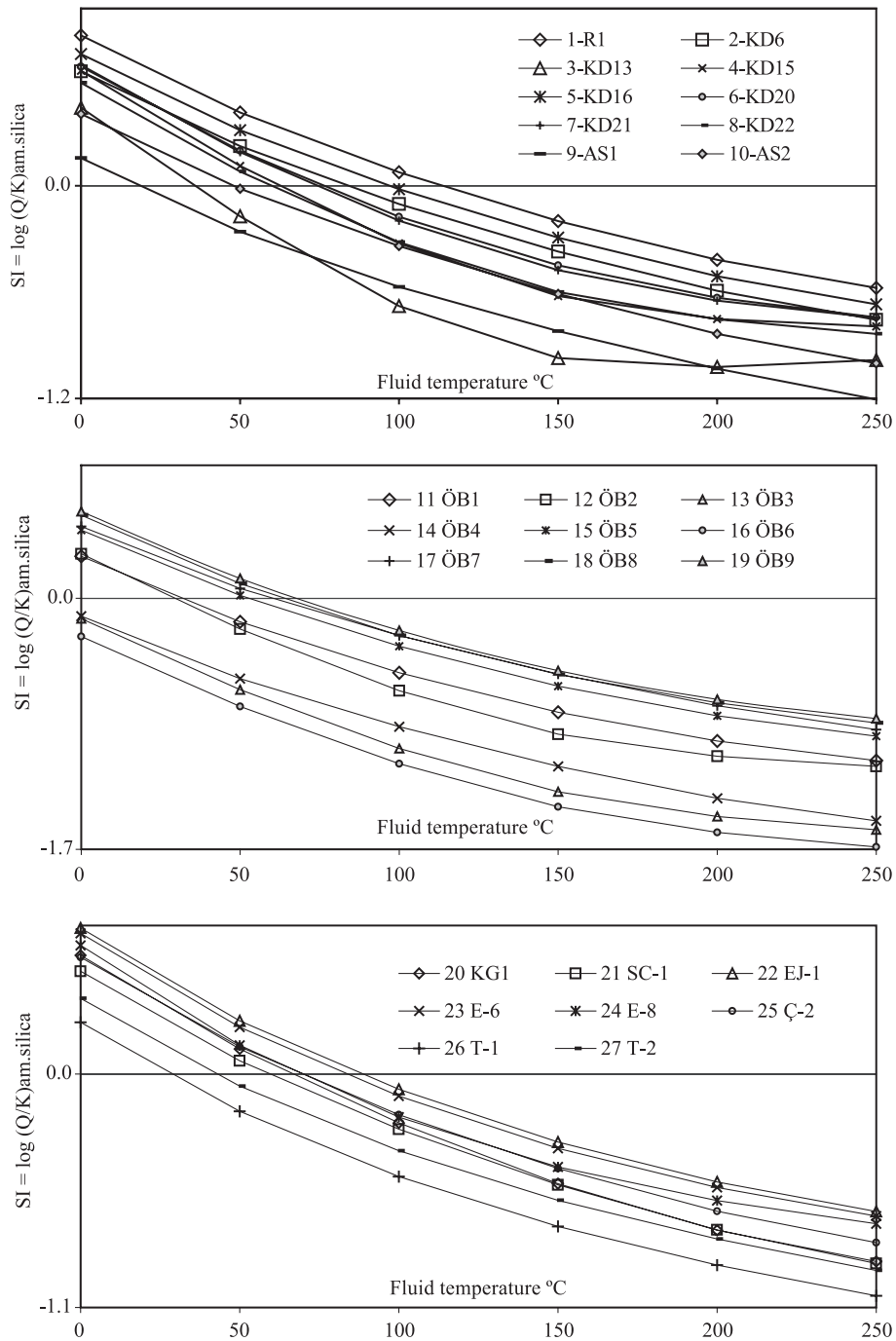


Fig. 7. Changes in the state of amorphous silica saturation in waters from selected geothermal wells in Turkey upon conductive cooling. Numbers are as Table 2.

phous silica show a reverse relationship in view of the mineral solubility and saturation properties.

Figs. 6 and 7 also show that, since both calcite and amorphous silica are undersaturated in the waters at 50–170 °C for Tuzla well T-2, 90–100 °C for Kızıldere wells KD-6 and R-1, respectively, an injection temperature at these temperature ranges is, therefore, recommended. The other wells show strong oversaturation with respect to calcite at any temperature and also show oversaturation with respect to amorphous silica below the temperature range 60–110 °C. Calcite precipitation just below the measured aquifer temperature seems to be inevitable, and there appears to be a second risk of amorphous silica scaling below 80 °C. Results for calcite and amorphous silica saturation states show that most of the geothermal well waters in Turkey are oversaturated with one or both minerals at all temper-

atures. It is considered most feasible to reinject all the geothermal well waters (>150 °C) of Turkey at the lowest temperature possible. Under these conditions, calcite oversaturation is minimal, and experience has shown that amorphous silica deposition, even from highly oversaturated solution, is very sluggish below about 50 °C.

## 5. Calculated aquifer chemistry

Version 2.1A of the WATCH (Bjarnason, 1994) chemical speciation program of Arnórsson et al. (1982) was used to assess aquifer chemistry and scaling properties of selected well waters in the principal geothermal areas of Turkey. All the well waters selected for this study have liquid enthalpy (the

Table 5

Calculated deep water composition (mg/kg) of thermal fluids from selected wells in primary Turkish geothermal areas, with steam loss at 100 °C assumed before sampling, using the boiling springs model of WATCH

Well No	Well Name	pH	SiO <sub>2</sub>	Na	K	Mg	Ca	B	F	Cl	SO <sub>4</sub>	Al	CO <sub>2</sub>	Steam loss fra.	Calc. <sup>a</sup> enthalpy
1	R-1	5.75	366	1101	147	0.036	0.38		18.8	95	380	1.732	65 587	0.278	1047
2	KD-6	5.21	253	925	107	0.223	0.94	16.3	14.1	37	525	0.122	75 201	0.184	834
3	KD-13	7.11	250	993	108	0.147	0.34		14.1	82	276	0.450	2549	0.182	830
4	KD-15	6.59	319	1065	123	0.192	0.76	21.6	18.7	47	562	0.199	5733	0.202	875
5	KD-16	5.47	309	978	119	0.229	2.87	21.2	18.7	39	516	0.236	62 203	0.214	902
6	KD-20	6.07	296	1072	113	0.121	1.29	19.3	18.1	113	545		11 855	0.194	857
7	KD-21	6.20	311	1246	113	0.193	1.45	20.1	16.9	113	621		9865	0.196	861
8	KD-22	6.30	254	1031	116	0.121	0.38		14.9	80	405	0.44	7829	0.196	861
9	AS-1	4.60	88.3	971	88	3.177	17.65	47.7	11.0	201	135		163 434	0.118	684
10	AS-2	5.10	154	949	78	0.949	12	36.3		201	147		75 563	0.137	728
11	ÖB-1	5.70	112	1087	36	12.8	40.0	36.0	1.957	1272	30		16 069	0.198	866
12	ÖB-2	6.44	119	1363	141		1.19	52.9	6.145	1012	53		8577	0.255	995
13	ÖB-3	6.22	41	1326	127	0.373	1.20	50.8	5.975	1358	55		11 395	0.253	990
14	ÖB-4	5.24	41	1110	105	1.329	9.38	43	5.668	1172	29		58 400	0.218	911
15	ÖB-5	5.74	160	1062	98	5.205	6.43	42.9		1113	35		24 691	0.235	948
16	ÖB-6	6.10	31	1359	138		2.76	56.7		1441	49		11 957	0.235	948
17	ÖB-7	5.10	172	882	106	4.89	15.24	44.9		686	41		94 420	0.198	866
18	ÖB-8	6.05	220	1190	11.5	186.5	6.14			1173	35		11 576	0.232	944
19	ÖB-9	5.89	217	1329	80	0.911	3.64	51.6	5.543	1381	100		19 540	0.241	962
20	KG-1	5.53	220	1710	67	2.615	10.8	73		139	1555	0.911	38 571	0.156	772
21	SC-1	5.16	192	609	63	5.466	37.6	60	2.778	103	30.5		37 655	0.104	654
22	EJ-1	5.64	321	446	48	4.315	10.2	2.37		70	415	0.3197	6296	0.119	689
23	E-6	5.73	309	472	55	5.141	5.67	0.96	0.366	71	404	0.322	4933	0.114	675
24	E-8	6.16	306	474	53	4.166	7.62	0.98		73	404	0.347	2035	0.094	632
25	Ç-2	5.18	221	362	34	4.942	22.95	0.13		57	347	0.094	17 314	0.116	684
26	T-1	3.94	106	19 118	1826	86.8	4912	30.9	3.695	37 928	227		3898	0.141	737
27	T-2	3.46	138	15 851	2422	59	2422	26.2	1.733	30 720	182		23 714	0.129	710

Sample numbers and names are the same as Table 2. Steam loss fra: Steam loss fraction; Calc. Enthalpy: calculated enthalpy.

<sup>a</sup> kJ/kg.

enthalpy of the well discharge is the same as that of liquid water at the aquifer temperature). The simplest case for assessing the aquifer fluid composition of geothermal wells occurs when the level of first boiling is within the well. This means that only liquid water exists in the aquifer. Accordingly, the enthalpy of the total well discharge and its composition is the same as those of the water entering the well (Arnórsson, 2000a,b,c). In terms of thermodynamics, the well is regarded as an isolated system (no mass and heat transfer), and the boiling is therefore adiabatic.

For wells selected in this study, the aquifer water composition was calculated on the basis that the enthalpy is equal to that of steam saturated water at the selected aquifer temperature. The pH in WATCH is calculated by considering all species of major components that can combine with  $H^+$ . For this purpose, measured aquifer temperatures were used, and the boiling temperature was accepted as 100 °C at which boiling is assumed to have occurred (100 cal/g). Table 5 gives the deep-water components, steam loss fractions, and calculated enthalpy values at the measured down hole temperature conditions. While all the major components diminish due to vaporization at 100 °C calculated alkalinity as  $CO_2$  (volatile component) increases.

## 6. Summary and conclusion

This study evaluates the state of mineral saturation and scaling tendencies in primary geothermal systems from Turkey using the chemical composition of well discharge waters, and measured and calculated reservoir temperatures. The areas include Kızıldere, Salavatlı, Germencik, Kavaklıdere-Sazdere, Salihli-Caferbeyli, Kütahya Simav, and Çanakkale Tuzla. Thermal waters in these geothermal systems circulate in metamorphic (marble, schist, quartzite, gneiss) and sedimentary rocks (limestone, conglomerate), except in Tuzla, which is hosted in granodiorite and volcanic rocks (rhyolite and latite). Thermal waters from selected wells are relatively dilute solutions except for Tuzla waters, which are extremely saline with Cl contents as high as 44 140 mg/kg. Measured temperatures of the systems are between 150 and 242 °C. Geothermometers compared with measured temperatures suggest that mixing and dilution occurred at

systems Salavatlı, Germencik, and Tuzla, and the main reservoir was not intersected at system Simav-Eynal. The Na–K–Mg diagram shows that Kızıldere waters are fully equilibrated, whereas the rest are immature to partial equilibrated.

All the wells selected for this study have liquid enthalpy. The aquifer water composition and speciation distribution were calculated with the aid of PhreeqCi and WATCH programs. For these calculations, the total discharge composition of the selected wells was taken to represent the aquifer water composition. The minerals include albite-low, amorphous silica, anhydrite, anorthite, aragonite, Ca-montmorillonite, calcite, celestite, chalcedony, dolomite, fluorite, gibbsite, gypsum, illite, kaolinite, K-feldspar, quartz, and strontianite. The aquifer waters are at near saturation with respect to three silica polymorphs, K-feldspar, dolomite, and strontianite. The waters, with some exceptions, are systematically oversaturated with respect to calcite, aragonite, and celestite, but undersaturated with respect to gypsum, anhydrite, fluorite, Ca-montmorillonite, anorthite, albite, gibbsite, illite, kaolinite. The highly saline Tuzla waters (T-1 and T-2) tend to be oversaturated in anhydrite, whereas the relatively dilute waters in other areas are undersaturated except for KG-1 waters. The calculated aquifer water compositions of the selected wells indicate that all the major components diminish upon adiabatic boiling (steam loss at 100 °C), except for  $CO_2$ , which increases.

Calcite and amorphous silica scaling tendencies in production wells were assessed in nine production well discharges. The results indicate that calcite-scaling tendencies in most wells are high from the onset of boiling to low temperatures. The boiled waters from most of the wells are oversaturated with respect to calcite even at low temperatures. The onset of potential deposition for amorphous silica is positively related to aquifer temperature, being ~120 °C for the hottest well (R-1) and less than ~80 °C for the cooler wells. Calcite and amorphous silica scaling tendencies in reinjection wells were also assessed for all the well discharges considered for this study. Most of the geothermal well waters in Turkey are oversaturated with one or both minerals at all temperatures. Assessment of calcite and amorphous silica scaling tendencies for selected well waters indicates that waste water disposal at most of the wells is most

feasible at the lowest possible temperature if scaling is to be minimized or avoided. Similarly, injection temperatures of about 100 and 150 °C are optimal for Kızıldere wells R-1 and KD-6 and Tuzla T-2, respectively.

## Acknowledgements

The author acknowledges the partial financial supports of Dokuz Eylül University Research Fund (Project number: 02.KB.FEN.059) and TÜBİTAK Research Fund (Project number: YDABAG-102Y039). Special thanks are due to my colleague Ünsal Gemici for his helpful suggestions. Critical reviews by Fraser Goff and an anonymous reviewer in an earlier version of this manuscript are gratefully acknowledged.

## References

- Ármannsson, H., 1989. Predicting calcite deposition in Krafla boreholes. *Geothermics* 18, 25–32.
- Árnórsson, S., 1989. Deposition of calcium carbonate minerals from geothermal waters—theoretical considerations. *Geothermics* 18, 33–39.
- Árnórsson, S., 2000a. Isotopic and chemical techniques in geothermal exploration, development and use: sampling methods, data handling, interpretation. International Atomic Energy Agency, Vienna (STI/PUB/1086, 351 pp.).
- Árnórsson, S., 2000b. The quartz and Na/K geothermometers. I. New thermodynamic calibration. Proceedings of WGC-2000 World Geothermal Congress, Japan, 28 May–10 June, Kyushu-Tohoku, pp. 929–934.
- Árnórsson, S., 2000c. The quartz and Na/K geothermometers: II. Results and application for monitoring studies. Proceedings of WGC-2000 World Geothermal Congress, Japan, 28 May–10 June, Kyushu-Tohoku, pp. 935–940.
- Árnórsson, S., Sigurdsson, S., Svavarsson, H., 1982. The chemistry of geothermal waters in Iceland: I. Calculation of aqueous speciation from 0 °C to 370 °C. *Geochim. Cosmochim. Acta* 46, 1513–1532.
- Bjarnason, J.O., 1994. The Speciation Program WATCH, version 2.1. Orkustofnun, Reykjavik, Iceland (7 pp.).
- Bozkurt, E., 2001. Neotectonics of Turkey—a synthesis. *Geodyn. Acta* 14, 3–30.
- Calmbach, L., 1997. AquaChem Computer Code-Version 3.7.42, Waterloo hydrogeologic. Waterloo, Ontario, Canada, N2L 3L3.
- Dora, O.Ö., Candan, O., Durr, S., Oberhansli, R., 1997. New evidence on the geotectonic evolution of the Menderes Massif. In: Pişkin, O., Savaşçın, M.Y., Ergün, M., Tarcan, G. (Eds.), Proceedings of International Earth Sciences Colloquium on the Aegean Region, 9–14 Oct. 1995, vol. 1, pp. 53–72.
- ENEL, 1989. Optimization and development of the Kızıldere geothermal field. ENEL, Aquater, DAL and Geotermica Italiana, Pisa, Italy, final report, 121 pp.
- Eşder, T., 1990. The crust structure and convection mechanism of geothermal fluids in Seferihisar geothermal area. In: Savaşçın, M.Y., Eronat, H. (Eds.), Proceedings of International Earth Sciences Congress on Aegean Regions, İzmir, Turkey, 1–6 Oct. 1990 vol. 1, pp. 135–147.
- Filiz, Ş., Tarcan, G., Gemici, Ü., 2000. Geochemistry of the Germencik geothermal fields, Turkey. Proceedings of WGC-2000 World Geothermal Congress, Japan, 28 May–10 June, Kyushu-Tohoku, pp. 1115–1120.
- Fournier, R.O., 1977. Chemical geothermometers and mixing models for geothermal systems. *Geothermics* 5, 41–50.
- Fournier, R.O., 1979. A revised equation for the Na–K geothermometer. *Trans. - Geotherm. Resour. Counc.* 3, 221–224.
- Fournier, R.O., Potter, R.W., 1979. Magnesium correction to the Na–K–Ca chemical geothermometer. *Geochim. Cosmochim. Acta* 43, 1543–1550.
- Fournier, R.O., Truesdell, A.H., 1973. An empirical Na–K–Ca geothermometer for natural waters. *Geochim. Cosmochim. Acta* 37, 1255–1275.
- Fytikas, M., Gialiani, O., Innocenti, F., Marinelli, G., Mazzuoli, R., 1976. Geochronological data on recent magmatism of the Aegean Sea. *Tectonophysics* 31, 29–34.
- Gemici, Ü., Tarcan, G., 2002. Hydrogeochemistry of the Simav geothermal field, western Anatolia, Turkey. *J. Volcanol. Geotherm. Res.* 116, 215–233.
- Giese, L.B., 1997. Geotechnische und umwelt geologische aspekte bei der forderung und reinjection von thermal fluiden zur nutzung geothermischer energie am beispiel des geothermal feldes Kızıldere und des umfeldes, W-Anatolien/Turkei (In German). PhD thesis, Freie Universität Berlin, 201 pp.
- Giese, L.B., Pekdeğer, A., Dahms, E., 1998. Thermal fluids and scalings in the geothermal power plant of Kızıldere, Turkey. In: Arehart, Ç., Hulston, J. (Eds.), Proceedings of the 9th International Symposium on Water–Rock Interaction, Taupo, New Zealand. Balkema, Rotterdam, pp. 625–628.
- Giggenbach, W.F., 1988. Geothermal solute equilibria. Derivation of Na–K–Mg–Ca geothermometers. *Geochim. Cosmochim. Acta* 52, 2749–2765.
- Giggenbach, W.F., 1991. Geochemical techniques in geothermal exploration. In: D'Amore, F. (Ed.), Application of Geochemistry in Geothermal Reservoir Development. UNITAR/UNDP publications, Rome, pp. 119–142.
- Gökgöz, A., 1998. Geochemistry of the Kızıldere–Tekkehamam–Buldan–Pamukkale geothermal fields, Turkey. UNU Geothermal Training Programme, Orkustofnun, Reykjavik, Iceland, Book of reports, 115–156.
- Karahan, Ç., Bakraç, S., Dünya, H., 2003. Alaşehir-Kavaklıdere-Göbekli jeotermal enerji araştırma sondajının (KG-1) değerlendirilmesi (In Turkish). In: Deliormanlı, A.H., Seçkin, C. (Eds.), Sondaj Sempozyumu MTA Ege Bölge Müdürlüğü ve TMMOB Maden Müh. Odası İzmir Şubesi, 10–11 Nisan 2002, Bildiriler, pp. 39–43.

- Karamanderesi, İ.H., 1986. Hydrothermal alteration in well Tuzla T-2, Çanakkale, Turkey. UNU Geothermal Training Programme, Reykjavik, Iceland. Book of Reports, 3–36.
- Karamanderesi, İ.H., 1997a. Geology and hydrothermal alteration processes of the Salavatlı-Aydın geothermal field. PhD thesis, Dokuz Eylül University, İzmir-Turkey, 238 pp.
- Karamanderesi, İ.H., 1997b. Salihli-Caferbeyli (Manisa İli) jeotermal sahası potansiyeli ve geleceği (In Turkish). Dünya Enerji Konseyi Türk Milli Komitesi, Türkiye, Enerji Kongresi teknik oturum bildiri metinleri, vol. 7, pp. 247–261.
- Karamanderesi, İ.H., Helvacı, C., 2003. Geology and hydrothermal alteration of the Aydın-Salavatlı geothermal field, western Anatolia, Turkey. Turk. J. Earth Sci. 12, 175–198.
- Kharaka, Y.K., Mariner, R.H., 1989. Chemical geothermometers and their application to formation waters from sedimentary basins. In: Naser, N.D., McCulloh, T.H. (Eds.), Thermal History of Sedimentary Basins; Methods and Case Histories Springer, pp. 99–117.
- Kristmannsdóttir, H., 1989. Types of scaling occurring by geothermal utilization in Iceland. Geothermics 18, 183–190.
- Líndal, B., Kristmannsdóttir, H., 1989. The scaling properties of the effluent water from Kızıldere power station, Turkey, and recommendation for a pilot plant in view of district heating applications. Geothermics 18, 217–223.
- MTA, 1996. Türkiye Jeotermal Envanteri (In Turkish). In: Erişen, B., Akkuş, İ., Uygur, N., Koçak, A. (Eds.), MTA Genel Müdürlüğü, Ankara (480 pp.).
- Mützenber, S., 1997. Nature and origin of the thermal springs in the Tuzla area, western Anatolia, Turkey. In: Schindler, C., Pfister, M. (Eds.), Active Tectonics of Northwestern Anatolia—The Marmara Poly-Project. A Multidisciplinary Approach by Space-Geodesy, Geology, Hydrogeology, Geothermics and Seismology. ETH, Zurich, pp. 301–320.
- Nicholson, K., 1993. Geothermal Fluids: Chemistry and Exploration Techniques. Springer-Verlag, Berlin Heidelberg (262 pp.).
- Parkhurst, D.L., Appelo, C.A.J., 1999. User's guide to PHREEQC (version 2)—a computer program for speciation, batch-reaction, one-dimensional transport, and inverse geochemical calculations: U.S. Geological Survey Water-Resources Investigations Report 99-4259, 312 pp.
- Satman, A., Uğur, Z., Onur, M., 1999. The effects of calcite deposition on geothermal well inflow performance. Geothermics 28, 425–444.
- Şamilgil, E., Arda, O., 1977. Laboratory analyses result of scale sample in Kızıldere. MTA report No. 9527, 1–8.
- Şener, M., Gevrek, A.İ., 2000. Distribution and significance of hydrothermal alteration minerals in the Tuzla hydrothermal system, Çanakkale, Turkey. J. Volcanol. Geotherm. Res. 96, 215–228.
- Şimşek, Ş., 1985. Geothermal model of Denizli-Saraykoy-Buldan area. Geothermics 14, 393–417.
- Şimşek, Ş., Yıldırım, N., 2000. İzmit ve Düzce depremlerinde jeotermal değişimler (in Turkish). Tübitak Bilim Tek. Derg. 387, 70–73.
- Şimşek, Ş., Doğdu, M.S., Akan, B., Yıldırım, N., 2000. Chemical and isotopic survey of geothermal reservoirs in Western Anatolia, Turkey. Proceedings of WGC-2000 World Geothermal Congress, Japan, 28 May–10 June, Kyushu-Tohoku, pp. 1765–1770.
- Tarcan, G., 2001. Aquifer chemistry and mineral saturation in selected high temperature geothermal areas. UNU Geothermal Training Programme, Orkustofnun, Reykjavik, Iceland. Book of Reports, 267–290.
- Tarcan, G., Gemici, Ü., 2003. Water geochemistry of the Seferihisar geothermal area, İzmir, Turkey. J. Volcanol. Geotherm. Res. 126, 225–242.
- Tarcan, G., Filiz, Ş., Gemici, Ü., 2000. Geology and geochemistry of the Salihli geothermal fields, Turkey. Proceedings of WGC-2000 World Geothermal Congress, Japan, 28 May–10 June, Kyushu-Tohoku, pp. 1829–1834.
- Tarcan, G., Gemici, Ü., Aksoy, N., 2002. İzmir İli sıcak ve mineralli kaynaklarının hidrojeoloji incelemesi. TÜBİTAK project, YDA-BAG-102Y039 (in Turkish; unpublished).
- Truesdell, A.H., 1976. Summary of section III geochemical techniques in exploration. Proceedings of Second United Nations Symposium on the Development and Use of Geothermal Resources. San Francisco, 1975 vol. 1. U. S. Government Printing Office, Washington D.C., pp. 53–89.
- Truesdell, A.H., Jones, B.F., 1974. WATEQ a computer program for calculating chemical equilibria of natural waters. J. Res. U.S. Geol. Surv. 2, 233–274.
- Vengosh, A., Helvacı, C., Karamanderesi, İ.H., 2002. Geochemical constraints for the origin of thermal waters from western Turkey. Appl. Geochem. 17, 163–183.
- Yıldırım, N., Demirel, Z., Doğan, A.U., 1997. Geochemical characteristics and re-injection of the Kızıldere-Tekkehamam geothermal field. In: Yilmazer, İ. (Ed.), Proceedings of GEO-ENV'97, International Symposium on Geology and Environment, 1–5 September, İstanbul-Turkey, pp. 48–55.
- Yılmaz, Y., Karacık, Z., 2001. Geology of the northern side of the Gulf of Edremit and its tectonic significance for the development of the Aegean grabens. Geodyn. Acta 14, 31–43.